



**HAL**  
open science

## Comparison of Heat Affected Zone due to nanosecond and femtosecond laser pulses using Transmission Electronic Microscopy

Ronan Le Harzic, Nicolas Huot, Eric Audouard, Christian Jonin, Pierre Laporte, Stéphane Valette, Anna Fraczkievic, Roland Fortunier

► **To cite this version:**

Ronan Le Harzic, Nicolas Huot, Eric Audouard, Christian Jonin, Pierre Laporte, et al.. Comparison of Heat Affected Zone due to nanosecond and femtosecond laser pulses using Transmission Electronic Microscopy. 2002. ujm-00118120

**HAL Id: ujm-00118120**

**<https://ujm.hal.science/ujm-00118120>**

Submitted on 4 Dec 2006

**HAL** is a multi-disciplinary open access archive for the deposit and dissemination of scientific research documents, whether they are published or not. The documents may come from teaching and research institutions in France or abroad, or from public or private research centers.

L'archive ouverte pluridisciplinaire **HAL**, est destinée au dépôt et à la diffusion de documents scientifiques de niveau recherche, publiés ou non, émanant des établissements d'enseignement et de recherche français ou étrangers, des laboratoires publics ou privés.

# Comparison of heat-affected zones due to nanosecond and femtosecond laser pulses using transmission electronic microscopy

R. Le Harzic,<sup>a)</sup> N. Huot, E. Audouard,<sup>b)</sup> C. Jonin, and P. Laporte

Laboratoire Traitement du Signal et Instrumentation (TSI), Université Jean Monnet, UMR CNRS 5516, 23 rue du docteur Paul Michelon, 42023 Saint Etienne cedex 2, France

S. Valette, A. Fraczkiewicz, and R. Fortunier

Ecole Nationale Supérieure des Mines, Centre SMS, 158 Cours Fauriel, 42023 Saint-Etienne cedex 2, France

(Received 13 December 2001; accepted for publication 28 March 2002)

This letter presents a method aimed at quantifying the dimensions of the heat-affected zone (HAZ), produced during nanosecond and femtosecond laser–matter interactions. According to this method, 0.1  $\mu\text{m}$  thick Al samples were microdrilled and observed by a transmission electronic microscopy technique. The holes were produced at laser fluences above the ablation threshold in both nanosecond and femtosecond regimes (i.e., 5 and 2  $\text{J}/\text{cm}^2$ , respectively). The grain size in the samples was observed near the microholes. The main conclusion is that a 40  $\mu\text{m}$  wide HAZ is induced by the nanosecond pulses, whereas the femtosecond regime does not produce any observable HAZ. It turns out that the width of the femtosecond HAZ is less than 2  $\mu\text{m}$ , which is our observation limit. © 2002 American Institute of Physics. [DOI: 10.1063/1.1481195]

Recent progress in femtosecond all solid-state laser technology enables fundamental and technological fields to be investigated. In particular, very precise processing of materials can be achieved.<sup>1,2</sup> It has been shown that the physical phenomena taking place during the laser–matter interaction depend strongly on the pulse duration, from the nanosecond (i.e., pulse duration  $>1$  ns) to the femtosecond (i.e., pulse duration  $<1$  ps) regime.<sup>3–5</sup> Among these phenomena, the present letter focuses on thermal effects during hole drilling or cutting. These thermal effects are due to the heat diffusion process and lead to a heat affected zone (HAZ) near the domain irradiated by the laser beam. In the nanosecond regime, typical 10  $\mu\text{m}$ –1 mm width HAZ are usually observed, whereas in the femtosecond case, due to the ultrashort pulse duration, the penetration length of thermal diffusion in the material is very limited, leading to a very small HAZ. The femtosecond regime is thus often considered as HAZ free, since the HAZ becomes very difficult to observe.

Studies on the thermal effects in the femtosecond regime are mainly theoretical, and concern the diffusion length along the beam axis.<sup>3,6,7</sup> Few experimental works have been published.<sup>8–10</sup> In this letter we focus on the dimension of the HAZ in the radial direction near microholes. In order to quantify these thermal effects, Al samples were fired with femtosecond and nanosecond pulses obtained from the same titanium–sapphire source. Transverse microstructural changes were analyzed by transmission electron microscopy (TEM). Indeed, such studies have already been initiated in the nanosecond regime.<sup>8</sup> We propose here a method for a quantitative analysis of the HAZ, and we give the obtained results by comparing the grain size evolution in the radial

direction for both nanosecond and femtosecond pulse duration.

The experimental setup is depicted in Fig. 1. Ultrashort laser pulses are generated by an amplified all solid-state Ti:sapphire laser chain. Low energy pulses are extracted from a mode-locked oscillator (1.6 nJ/pulse, 80 MHz, 800 nm, 120 fs). The pulses are then injected in an amplifying chain including: an optical pulse stretcher, a regenerative amplifier associated with a two-pass amplifier using as pumping source, a 20 W Nd:YLF laser, and a pulse compressor.

P-polarized pulses with the wavelength centered around 800 nm, an energy of 1.5 mJ, and a 1 kHz repetition rate with a typical duration of 150 fs are obtained. Nanosecond pulses are extracted from the same regenerative amplifier without any fs pulses injection from the oscillator. The pulse duration obtained is then within the range of 7–8 ns.

To allow a low energy regime (typically 0.01–0.5 mJ/

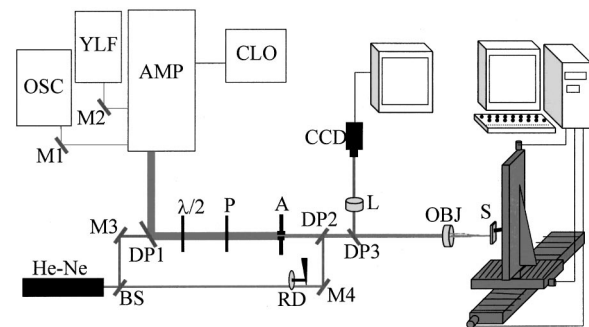


FIG. 1. Experimental setup: (OSC) femtosecond oscillator 80 MHz, 1.6 nJ/pulse, 120 fs; (YLF) flash-pumped ns 20 W 1 kHz Nd:YLF laser; (AMP) stretcher, regenerative amplifier and compressor (1.5 mJ/pulse, 1 kHz, 150 fs); (CLO) external controlled clock device; He–Ne: cw 4 mW He–Ne laser for alignment and imaging; (BS) beam sampler; ( $M_i$ ) mirrors; (A) circular aperture; ( $DP_i$ ) dichroic plate; (P) polarizer; (HW) half-wave plate; (L) lens; (OBJ) focusing objective; (RD) rotating diffusing plate; (S) sample; and ( $MT_i$ ) motorized translations.

<sup>a)</sup>Author to whom correspondence should be addressed; electronic mail: leharzic@univ-st-etienne.fr

<sup>b)</sup>Electronic mail: audouard@univ-st-etienne.fr

pulse), laser pulses are obtained without using the two-pass amplifier. Additional attenuation is then provided by a half-wave plate coupled with a polarizer. An external electronic clock device, which controls the voltage applied to the Pockels cell, also allows the use of this system in a single shot mode.

The samples are mounted on a three-motorized-axes system with  $0.5 \mu\text{m}$  accuracy. Focusing objectives of 25 or 10 mm focal lengths were used to obtain microholes with a diameter less than  $100 \mu\text{m}$ . Experiments are performed at the image point of a 3.5 mm aperture placed 1.35 m before the objective so that borders and spurious conical drilling effects are reduced. The drilling process is monitored in real time thanks to an incoherent imaging system with a less than  $5 \mu\text{m}$  resolution, which is wide enough compared to typical microholes dimensions.

The Al samples used in this study are to be observed with a TEM. The experimental procedure proposed here is based on a laser drilling of samples previously prepared for TEM analysis. Thus the thickness of the samples is first reduced down to  $500 \text{ nm}$  before laser processing. This allows for a local study of the effects produced by a finite number of low fluence laser pulses. In this study, 1000 pulses were produced in 1 s with fluences of 2 and  $5 \text{ J/cm}^2$ , respectively, for the femtosecond and the nanosecond cases. These fluences were chosen above the ablation threshold in both cases. As mentioned above the drilling is performed at the image point and due to the thinness of the sample, the number of incident pulses (10–1000) has no significant effect as experimentally determined.

The thickness of the samples was reduced by an electrolytic process. Metallic disks of about 3 mm in diameter were used. The process was stopped automatically when light was detected through the sample. It turns out that a randomly shaped hole is always present in the middle of the sample. Throughout this letter, this hole will be referred to as the “middle hole.”

The thickness of the area observed by a CM 200 TEM operated at 200 kV used in this study has to be less than  $500 \text{ nm}$ . This area is thus located in the vicinity of the thinned down hole, namely at a maximum distance of  $40\text{--}100 \mu\text{m}$ , depending on the quality of the thinning down. In order to observe the local effects induced by laser drilling, the produced holes have to cross this area. Positioning of the target sample was achieved by using the realtime imaging device described above.

As already mentioned in the literature,<sup>2,11</sup> metal melting and matter redeposition occur in the nanosecond regime. In the femtosecond case no damage is observed. It turns out that ultrashort laser pulses are then usually said to produce no thermal effects. Only qualitative conclusions can be deduced from optical observations, since the HAZ cannot be accurately measured. In order to obtain a quantitative estimation of the HAZ width, we focused on the evolution of the grain size between the middle and the laser drilled holes. Indeed, by a physical metallurgy approach, one can directly correlate the grain size modification to the temperature.<sup>12</sup> Typically, our samples have a polycrystalline structure, constituted by the juxtaposition of monocrystal grains separated by grain boundaries. Each grain has its own orientation. The grain

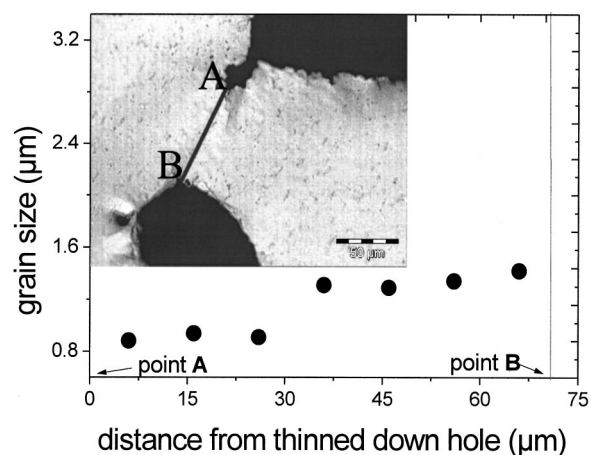


FIG. 2. Evolution of the grain size in the sample drilled with nanosecond pulses. Optical microscope top view ( $\times 50$ ), shows the thinned down hole (point A) and the laser hole (point B).

boundaries linking the different oriented grains have a positive interfacial energy. This polycrystalline system does not have a state of minimum energy. A perfect crystal, in thermodynamic equilibrium, would have no grain boundaries. An energy supply through a temperature increase yields a thermal activation, minimizing the energy of the crystal, leading to a grain size growth. Thus the grain size evolution provides an accurate signature of the thermal history of the sample and, as a consequence, the spread of the HAZ. To obtain the local grain size, the images obtained by TEM were treated by an average statistical method.

Figure 2 displays the evolution of the grain size in the sample, which is drilled with nanosecond pulses. Several images were analyzed between point A (“middle hole” border) and point B (laser hole border). Two regions can be observed. In the vicinity of the middle hole, up to  $35 \mu\text{m}$  from it, the grain size is approximately  $0.9\text{--}1.0 \mu\text{m}$ , which is the initial grain size of the sample. The second region, near the laser hole, is characterized by a grain growth. In this region, the grain size increases up to  $1.3\text{--}1.4 \mu\text{m}$ . The transition between these two regions gives the size of the HAZ. In the nanosecond regime, the HAZ is then about  $40 \mu\text{m}$  in width.

Figure 3 represents the grain size evolution between the

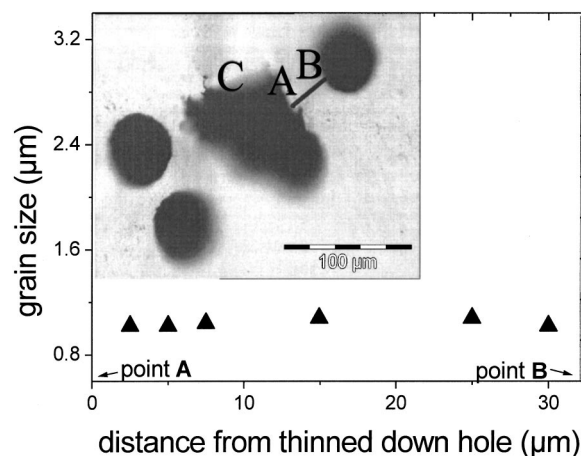


FIG. 3. Evolution of the grain size in the sample drilled with femtosecond pulses. Optical microscope top view ( $\times 50$ ), shows the thinned down hole (point A) and the laser hole (point B).

middle hole (point *A*) and the laser hole (point *B*) in the case of femtosecond pulses. In this case, only one region can be identified, with a constant grain size of about 1  $\mu\text{m}$ . Since the distance between points *A* and *B* is only 35  $\mu\text{m}$ , the grain size was also determined at point *C*, which is located far from the laser holes. A 1  $\mu\text{m}$  grain size was also obtained at this point. As a consequence, we determined that the size of the HAZ is less than 2  $\mu\text{m}$  in the femtosecond regime. This value corresponds to the nearest position from the laser hole border that could be analyzed.

In a previous work using the TEM technique, the width of the HAZ was found to be independent of the pulse duration (from 50 ns to 200 fs),<sup>8</sup> and reached a value of 5–10  $\mu\text{m}$ . It should be noticed here that these results, which are not in agreement with the present work, were obtained with very different experimental conditions (very high fluences, thick samples, etc).

The experimental procedure presented in this letter emphasizes the different HAZ sizes obtained with nanosecond and femtosecond regimes, which was evidenced by many theoretical investigations.<sup>3,4,13,14</sup> According to these studies, the HAZ is due to the smaller value of the electron specific heat compared to the lattice one. In the femtosecond regime, the energy brought by optical excitation is mainly deposited into the electron bath. This bath is then cooled by electron–phonon coupling, leading to a heating of the lattice up to melting. At this point, the diffusion of the electrons is considered to be stopped and the HAZ is then defined as the corresponding diffusion length. This length is found to be a few hundreds of nanometers in the case of metals. A thermal model is currently used to describe the heat diffusion in the sample, and thus explains the differences between nanosec-

ond and femtosecond regimes. Such results for the radial thermal diffusion length are in progress and will be published in a forthcoming article.

The authors thank the European Community (FEDER funds 1997/1999), the Conseil Général de la Loire en Rhône-Alpes, and Saint-Etienne Métropole for financial support.

<sup>1</sup>X. Zhu., *Appl. Surf. Sci.* **167**, 230 (2000).

<sup>2</sup>C. Momma, B. N. Chichkov, S. Nolte, F. von Alvensleben, A. Tunnermann, H. Welling, and B. Wellegehausen, *Opt. Commun.* **129**, 134 (1996).

<sup>3</sup>P. B. Corkum, F. Brunel, N. K. Sherman, and T. Srinivasan-Rao, *Phys. Rev. Lett.* **61**, 2886 (1988).

<sup>4</sup>B. N. Chichkov, C. Momma, S. Nolte, F. von Alvensleben, and A. Tunnermann, *Appl. Phys. A: Mater. Sci. Process.* **63**, 109 (1996).

<sup>5</sup>S. Nolte, C. Momma, H. Jacobs, A. Tunnermann, B. N. Chichkov, B. Wellegehausen, and H. Welling, *J. Opt. Soc. Am. B* **14**, 2716 (1997).

<sup>6</sup>S.-S. Wellershoff, J. Hohlfeld, J. Güdde, and E. Matthias, *Appl. Phys. A: Mater. Sci. Process.* **A 69**, 99 (1999).

<sup>7</sup>A. P. Kanavin, I. V. Smetanin, V. A. Isakov, Y. V. Afanasiev, B. N. Chichkov, B. Wellegehausen, S. Nolte, C. Momma, and A. Tunnermann, *Phys. Rev. B* **57**, 14698 (1998).

<sup>8</sup>N. K. Sherman, F. Brunel, P. B. Corkum, and F. A. Hegmann, *Opt. Eng.* **28**, 1114 (1989).

<sup>9</sup>A. Luft, U. Franz, A. Emsermann, and J. Kaspar, *Appl. Phys. A: Mater. Sci. Process.* **A 63**, 93 (1996).

<sup>10</sup>P. S. Perry, *Laser Surface Treatment of Metals*, edited by C. W. Draper and P. Mazzoldi, (Dordrecht, Netherlands, 1986), p. 57.

<sup>11</sup>X. Zhu, A. Naumov, D. Villeneuve, and P. Corkum, *Appl. Phys. A: Mater. Sci. Process.* **A 69**, 1 (1999).

<sup>12</sup>See for instance J. D. Verhoeven, *Fundamentals of Physical Metallurgy*, (Wiley, New York, 1975); P. Haasen, *Physical Metallurgy*, 3rd ed. (Cambridge University Press, Cambridge, 1996).

<sup>13</sup>S. I. Anisimov, B. L. Kapeliovich, and T. L. Perel'man, *Sov. Phys. JETP* **39**, 375 (1974).

<sup>14</sup>M. I. Kaganov, I. M. Lifshitz, and L. V. Tanatarov, *Sov. Phys. JETP* **4**, 173 (1957).